

# A thermally sensitive energy-absorbing composite functionalized by nanoporous carbon

Weiyi Lu and Venkata K. Punyamurtula

*Department of Structural Engineering, University of California—San Diego, La Jolla, California 92093-0085*

Aijie Han

*Department of Chemistry, University of Texas—Pam America, Edinburg, Texas 78539*

Taewan Kim

*Program of Materials Science & Engineering, University of California—San Diego, La Jolla, California 92093*

Yu Qiao<sup>a)</sup>

*Department of Structural Engineering, University of California—San Diego, La Jolla, California 92093-0085; and Program of Materials Science & Engineering, University of California—San Diego, La Jolla, California 92093*

(Received 30 April 2009; accepted 21 July 2009)

A polypropylene-matrix composite material functionalized by nanoporous particulates was produced. When the temperature is relatively low, the matrix dominates the system behavior. When the temperature is relatively high, with a sufficiently large external pressure the polymer phase can be intruded into the nanopores, providing an energy absorption mechanism.

## I. INTRODUCTION

Composite materials, especially polymer matrix composites, have been intensively studied for energy absorption applications.<sup>1</sup> When the temperature is close to or higher than the glass transition temperature ( $T_g$ ), the polymer matrix is usually viscoelastic. With an external loading, either dynamic or quasi-static, the relaxation of the network polymer chains would cause a considerable energy dissipation effect, which works quite well under cyclic loadings.<sup>2</sup> The reinforcements can be continuous fibers, short fibers, particulates, and/or platelets.<sup>3–5</sup> They can significantly enhance the overall stiffness, strength, and toughness, as well as the anisotropic and heterogeneous properties.<sup>6</sup> If the bonding between the matrix and the reinforcements is relatively weak, debonding can take place when the local stress exceeds the critical value, which is often promoted by the stress concentration and/or wave redispersion.<sup>7</sup> As a first-order estimation, debonding of reinforcements of an overall interfacial area of  $A$  would result in an energy dissipation of

$$E = \gamma_d \cdot A \quad , \quad (1)$$

where  $\gamma_d$  is the effective surface free energy.

It can be seen that if the interfacial area,  $A$ , increases, the theoretical upper limit of the energy absorption capacity is higher, and thus using nanometer (nm)-sized

fillers of ultralarge surface to volume ratios becomes an attractive concept.<sup>8</sup> For instance, if 1 g of carbon nanotubes (CNTs) are embedded in a polymer matrix and if they can fully debond,  $10^2$  to  $10^3$  Joules (J) of energy can be dissipated. The high stiffness and strength of CNTs assure that they have the ability to store sufficient strain energy to trigger the interface debonding.

However, under a compressive loading, especially when the strain rate is high, debonding would inevitably cause local weakening, which makes the stress wave distribution highly nonuniform.<sup>9</sup> As a result, shear localization can significantly limit the overall energy absorption efficiency. In a few narrow shear bands, local deformation can rapidly develop, and catastrophic failure may happen without bulk-distributed damages; i.e., the large interface area cannot be fully used.<sup>10</sup> This embrittlement effect has become a major challenge that must be overcome before nanocomposites can be widely applied in engineering practice. Moreover, while interface debonding can occur relatively easily under a tensile or shear stress; in a compressive stress field it can be difficult.

Recently, we investigated another type of nanocomposite—nanoporous materials functionalized (NMF) material.<sup>11–14</sup> The matrix must be a liquid or a gel, which is flowable under an external loading. The fillers are nanoporous particles. The particle size can be large, in the range of a fraction of micrometers ( $\mu\text{m}$ ) to a few millimeters (mm). The particles contain large volume fractions of nm-sized pores, with a pore size of 0.6 to

<sup>a)</sup>Address all correspondence to this author.

e-mail: yqiao@ucsd.edu  
DOI: 10.1557/JMR.2009.0408

100 nm. Although the outer surface area is relatively small, the area of the nanopore inner surface is ultra-large, usually  $10^2$  to  $10^3$  m<sup>2</sup> per gram. Appropriate surface treatment should be performed so that the inner surfaces are nonwettable to the liquid/gel phase. Thus, only when the liquid/gel phase is subjected to a relatively large compressive stress, can the capillary effect be overcome and liquid infiltration take place, associated with a large increase in system free energy:

$$E = \Delta\gamma \cdot A_i \quad , \quad (2)$$

where  $\Delta\gamma$  is the excess solid–liquid interfacial tension and  $A_i$  the nanopore inner surface area. The value of  $\Delta\gamma$  is typically 10–100 mJ/m<sup>2</sup>. Consequently, the energy absorption capacity of an NMF material is 1 to 10<sup>2</sup> J/g. Experimental data have shown that due to the uniform distribution of the loading in the liquid/gel phase the entire nanopore surface can be accessed.<sup>12</sup>

One difficulty associated with the NMF materials technique is that the liquid phase must be contained in a packaging system, either a cellular or a vascular structure, which increases the system complexity. Although hydrogel matrix NMF composites have been developed,<sup>15,16</sup> they can merely stand alone and still cannot be directly used for load-bearing components.

When a material is subjected to intense stress waves, due to the small time scale of deformation, the dissipated energy cannot be transported and thus the local temperature can greatly increase by a few hundred °C in a short period of time, which may cause melting of polymers and even metals.<sup>17</sup> The energy dissipation can be caused by debonding, cell buckling, internal friction, etc.,<sup>18</sup> or by the shock viscosity effect, which is related to the irreversibility of loading and unloading paths.<sup>19</sup> It is envisioned that if a nanoporous phase is embedded in a composite the softened materials, e.g., a low melting point polymer, may be intruded into the nanopores. The small mass density of the nanoporous phase also helps with reducing the overall weight. However, flow of viscous materials in a confining nanoenvironment may be difficult. Currently, little experimental data are available in open literature.

## II. EXPERIMENTAL

In the current study, we investigated a Cabot BP-2000 nanoporous carbon. It is a lightweight material with a particle size of 10 to 100 μm. The material was dried in air at 80 °C for 2 h, and heated in a tube furnace in a nitrogen environment at 550 °C for 6 h. After rinsing in acetone and warm water repeatedly, the carbon sample was soaked with saturated water steam at 180 °C for 12 h. The steam flow rate was maintained at 30 mL/min. After vacuum drying at 80 °C for 4 h, 2.5 g of carbon was mixed with 40 mL of dry toluene in a round-bottom flask.

The mixture was gently stirred for 10 min, and during this time 1 mL of chlorotrimethylsilane was injected. The temperature was then increased to 95 °C by a thermal mantle and the mixture was vigorously stirred for 48 h. The silane-treated material was filtered, washed with dry toluene and warm water repeatedly, and dried in vacuum at 80 °C for 6 h. The nanoporous structure was characterized in a Micromeritics ASAP-2000 analyzer (Norcross, GA), as shown in Figs. 1 and 2.

The surface-treated nanoporous carbon was mixed with polypropylene (PP) pellets, with a mass ratio of 1:20. By using a heating plate, PP was melted and the mixture was blended at 200 rpm for 10 min, so that the carbon particles dispersed uniformly, and then at 10 rpm

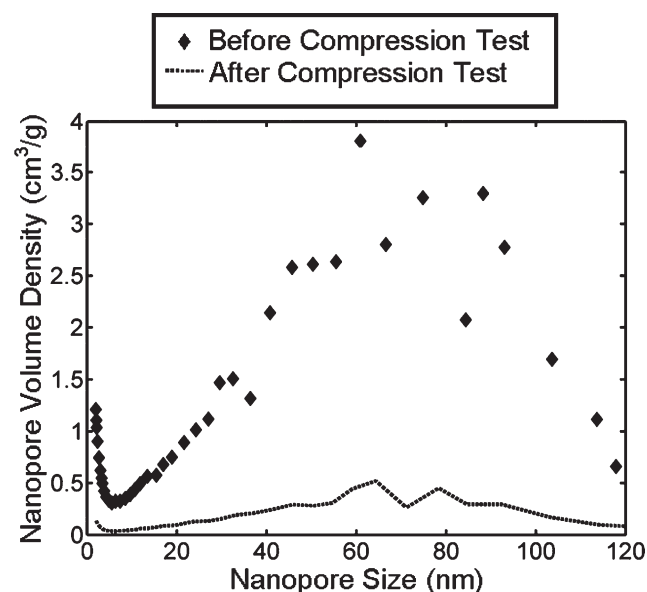


FIG. 1. The nanopore volume distributions (a) before and (b) after the compression test.

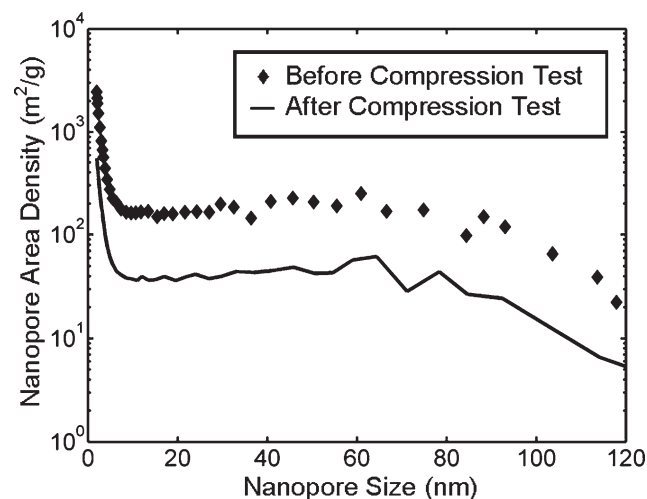


FIG. 2. The nanopore surface area distributions (a) before and (b) after the compression test.

for 10 min, so that the content of entrapped air was minimized. The mixture was cooled in air, forming a PP matrix composite, and cut into cylinders with a diameter of 19 mm.

In a stainless steel cylinder, a PP composite cylinder was sealed from the top by a stainless steel piston. The cross-sectional area of the piston was 286 mm<sup>2</sup>. The sealing was assured by two reinforced teflon o-rings. The testing temperature was controlled by an oil bath either at room temperature (20 °C) or at an elevated temperature (280 °C). In a type 5580 Instron machine (Norwood, MA), the piston was compressed into the cylinder at a constant rate of 0.5 mm/min. When the load reached about 700 N, the piston was moved at a rate of -0.5 mm/min. Similar loading-unloading cycles were repeated two times. Figure 3 shows typical compression isotherm curves.

After the compression test, the composite was cooled in air, milled into powders, and washed and filtered in acetone and methanol repeatedly until about 20 mg of carbon particles were collected. The collected carbon powders were characterized again in the Micromeritics ASAP-2000 analyzer.

### III. RESULTS AND DISCUSSION

Figure 1 clearly shows that before the compression test the nanopore volume followed a bimodal distribution. The higher peak is at about 60 nm and the lower peak is at about 2 nm. Figure 2 shows that although the small nanopores are of a relatively low volume fraction, their surface area is large, as it should be, since the surface area is proportional to  $V/d$ , with  $V$  being the characteristic volume and  $d$  being the characteristic size. The nanopore volume density at the lower peak is about

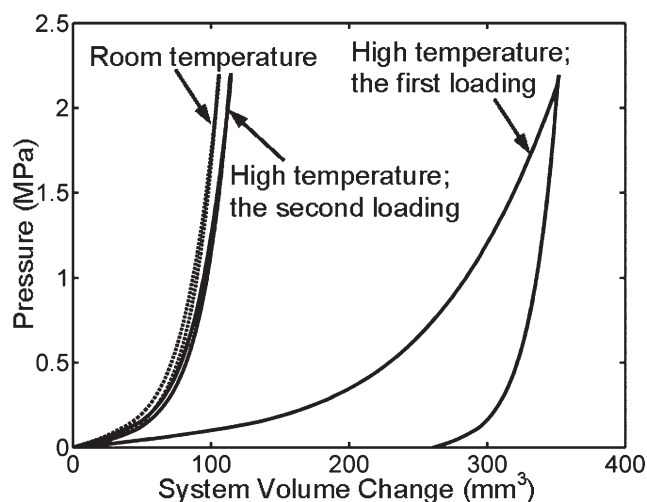


FIG. 3. Typical compression curves. The dashed curve is for the system performance at room temperature and the solid curves are for the system performance at elevated temperature.

one-third of that at the higher peak, and the nanopore area density of the former is nearly 10 times larger.

The dashed lines in Fig. 3 indicate the system behavior at room temperature, which is linear. The compressibility is determined by the bulk modulus of the composite material and the compliance of the loading machine. At a peak load of 700 N, the pressure is around 2.2 MPa. In this pressure range, no plastic deformation takes place in both the PP phase and the carbon phase, and therefore the loading and unloading paths nearly overlap with each other.

The melting point of PP is  $T_m = 160$  °C. It is softened when the temperature is increased to 280 °C. At this temperature, as the external pressure is applied a large deformation occurs. Since the compressibility of the liquid phase is even smaller than its solid counterpart,<sup>20</sup> the deformation must be attributed to the infiltration of PP melt into the nanopores, as depicted in Fig. 4. The inner surface of nanopores of the BP2000 under investigation is coated by a silane monolayer, which is nonwettable to the PP macromolecules.<sup>21</sup> When the carbon particles and the PP melt are mixed under ambient pressure, the PP chains would stay outside the nanopores to minimize the system free energy. Above  $T_m$ , the free volume among the PP chains greatly increases and can relatively easily slide against each other. As the piston is compressed into the cylinder, strain energy builds up in the PP matrix:  $U = P^2/2B$ , where  $P$  is the pressure and  $B$  is the effective bulk modulus. When the PP chains enter the nanopores, the system free energy increases by  $U_1 = \Delta\gamma \cdot A_i$ , where  $A_i = 2/r$  is the specific contact area, with  $r$  being the effective nanopore radius. When  $U$  and  $U_1$  are balanced by each other, the equilibrium condition is reached, at which  $P = \sqrt{4B \cdot \Delta\gamma / r}$ . According to the measured curve,  $P$  is in the range of 0.05 to 2 MPa. The average infiltration pressure is about 1 MPa. If the corresponding pore size is taken as the higher modal value, 60 nm, the value of  $\Delta\gamma$  can be estimated as 600 mJ/m<sup>2</sup>, with the value of  $B$  being set to 2500 MPa. This value of interfacial tension is relatively large compared with that of a carbon-water system,<sup>22</sup> compatible with the fact that the surface tension of PP melt is larger.

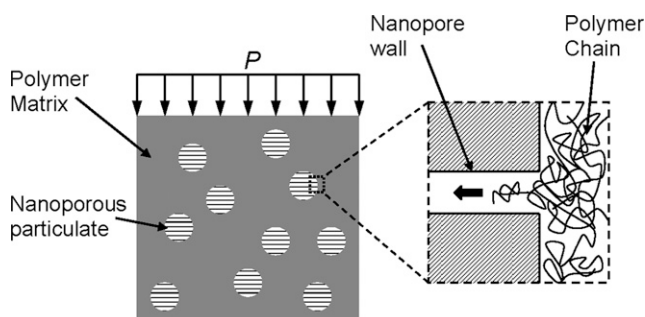


FIG. 4. Schematic of the thermally sensitive composite functionalized by nanoporous carbon.

When unloading begins, the slope of the sorption isotherm curve is quite large and does not decrease until the pressure is relatively low. When  $P$  is 0.2 MPa, the slope is reduced by nearly 50%. As  $P$  is entirely removed, there is still a significant amount of residual deformation of about  $270 \text{ mm}^3$ . Clearly, the confined PP melt does not defiltrate, and thus the sorption isotherm curve is highly hysteretic. The nondefiltration may be related to the large aspect ratio of the nanopores, where the liquid phase in the middle section may be regarded as confined in an infinitely long channel. Under this condition, the driving force of defiltration associated with the positive interfacial tension is balanced. The difficulty in formation and growth of nanobubbles can also lead to the blocking of confined matters, especially when the nanopore size is larger than 1–2 nm.<sup>23,24</sup>

At the second loading, the loading and unloading paths are nearly identical, both of which are similar to the unloading section of the first loading. The slope is close to that at the high-pressure segment, suggesting that no infiltration or defiltration is involved. It is clear that as the nanopores remain occupied the system compressibility is relatively small; i.e., the infiltration mechanism works only in the first loading loop, suitable to one-time protection applications. After the first loading cycle, the nanoporous carbon particulates are strongly bonded with the matrix by the penetrating PP phase.

According to Figs. 1 and 2, the porosity changes significantly after the compression test. After the test, the peak in the larger nanopore size range vanishes. The relatively small residual nanopore volume may be caused by the loss of confined PP during the filtering and washing process. The peak of the smaller nanopore size, although considerably lowered, is still evident. That is, most of the smallest nanopores of the sizes around 1–2 nm remain empty. If they were filled by the PP phase during loading and the confined PP macromolecules defiltrated during unloading, associated with the significantly different nanopore sizes of the two peaks, the infiltration plateau in Fig. 3 would contain two stages, which is not observed in the experiment. If the excess interfacial tension is at the same level in the small and large nanopores, the infiltration pressure in the smallest nanopores should be higher than that of the large nanopores by 30 to 60 times, beyond the capacity of the current system. In fact, under such a high pressure, the nanoporous carbon particulates can be crushed, which is another possible energy absorption mechanism but not the focus of the current study.

It is clear that a number of important questions, e.g., (i) what is the effect of the nanopore size on polymer intrusion, (ii) are nominal melting points the same inside and outside nanopores, (iii) what would be the loading

rate effect, etc., remain unanswered. These questions will be the focus of our future investigation.

#### IV. CONCLUDING REMARKS

Through a compression experiment, it has been validated that as nanoporous carbon particulates are embedded in a polypropylene matrix, at an elevated temperature the polymer phase can be forced into the nanopores, leading to a significant energy dissipation effect. As the pressure is lowered, the confined polymer chains do not defiltrate. The accessible nanopores are of relatively large sizes. In the smallest nanopores around 1–2 nm, in the pressure range of the current study, infiltration does not occur.

#### ACKNOWLEDGMENT

This study was supported by the National Science Foundation and The Sandia National Laboratory under Grant No. CMS-0623973.

#### REFERENCES

1. E.J. Barbero: *Introduction to Composite Materials Design* (Taylor & Francis, Philadelphia, PA, 1999).
2. H.F. Brinson and L.C. Brinson: *Polymer Engineering Science and Viscoelasticity* (Springer, New York, 2008).
3. A.R. Bunsell: *Fiber Reinforcements for Composite Materials* (Elsevier, New York, 1988).
4. S. Mazumdar: *Composites Manufacturing: Materials, Product, and Process Engineering* (CRC Press, Boca Raton, FL, 2002).
5. T.J. Pinnavaia and G.W. Beall: *Polymer-Clay Nanocomposites* (John Wiley & Sons, New York, 2000).
6. I.S. Daniel and O. Ishai: *Engineering Mechanics of Composite Materials* (Oxford University Press, New York, 1994).
7. G. Lu and T. Yu: *Energy Absorption of Structures and Materials* (Woodhead Publishing, Abington, UK, 2003).
8. T.E. Twardowski: *Introduction to Nanocomposite Materials* (Destech Publishing, Lancaster, PA, 2007).
9. H.S. Park and W.K. Liu: An introduction and tutorial on multiple scale analysis in solids. *Comput. Methods Appl. Mech. Eng.* **193**, 1733 (2004).
10. X. Kong, S.S. Chakravarthula, and Y. Qiao: Evolution of collective damage in a polyamide 6-silicate nanocomposite. *Int. J. Solids Struct.* **43**, 5969 (2006).
11. A. Han, V.K. Punyamurtula, T. Kim, and Y. Qiao: The upper limit of energy density of nanoporous materials functionalized liquid. *J. Mater. Eng. Perform.* **17**, 326 (2008).
12. F.B. Surani and Y. Qiao: An energy absorbing polyelectrolyte gel matrix composite material. *Composites Part A* **37**, 1554 (2006).
13. A. Han, V.K. Punyamurtula, and Y. Qiao: Infiltration of liquid metals in a nanoporous carbon. *Philos. Mag. Lett.* **88**, 67 (2008).
14. A. Han, V.K. Punyamurtula, and Y. Qiao: Effects of decomposition treatment temperature on infiltration pressure of a surface modified nanoporous silica gel. *Chem. Eng. J.* **139**, 426 (2008).
15. F.B. Surani, A. Han, and Y. Qiao: Thermal recoverability of a polyelectrolyte modified, nanoporous silica based system. *J. Mater. Res.* **21**, 2389 (2006).

16. F.B. Surani and Y. Qiao: Energy absorption of a polyacrylic acid partial sodium salt modified nanoporous system. *J. Mater. Res.* **21**, 1327 (2006).
17. V. Nesterenko: *Dynamics of Heterogeneous Materials* (Springer, New York, 2001).
18. A. Han, V.K. Punyamurtula, and Y. Qiao: Heat generation associated with pressure induced infiltration in a nanoporous silica gel. *J. Mater. Res.* **23**, 1902 (2008).
19. N. Yoganandan, J. Zhang, and F. Pintar: Force and acceleration corridors from lateral head impact. *Traffic Inj. Prev.* **5**(4), 368 (2004).
20. M. Kleman and O.D. Lavrentovich: *Soft Matter Physics* (Springer-Verlag, New York, 2003).
21. H. Ibach: *Physics of Surfaces and Interfaces* (Springer-Verlag, Berlin, 2006).
22. A. Han and Y. Qiao: Controlling infiltration pressure of a nanoporous silica gel via surface treatment. *Chem. Lett.* **36**, 882 (2007).
23. Y. Qiao, G. Cao, and X. Chen: Effects of gas molecules on nanofluidic behaviors. *J. Am. Chem. Soc.* **129**, 2355 (2007).
24. Han A, Kong X, Qiao Y. Pressure induced infiltration in nanopores. *J. Appl. Phys.* **100**, 014308 (2006).